Improvement of finite difference methods for step-index optical waveguides

C. Vassallo

Indexing terms: Waveguides and waveguide components, Modelling

Abstract: New 3-point finite difference formulae with equally spaced grid points are given for the analysis of scalar or semivectorial fields in waveguides with discontinuous refractive index profiles. The new formulae lead to more accurate calculations for the modes than the previously known methods, irrespective of the location of the discontinuities with respect to the grid points and without averaging the permittivity over meshes.

1 Introduction

Finite difference methods are attractive techniques to analyse the fields in arbitrarily shaped optical systems. They are simple to program and because they involve calculations with sparse matrices, they make efficient use of computer memory. The most elementary of them are based on the classical 3-point formula

$$\frac{\partial^2\psi(x)}{\partial x^2} = \frac{1}{h^2}[\psi(x+h) + \psi(x-h) - 2\psi(x)] + O(h^2) \quad (1)$$

The notation $O(h^2)$ means that terms of order h^2 are neglected or, equivalently, that the formula is exact up to the first-order in h. It is not always emphasised that this formula implies that the second derivative must be continuous within $(x-h, x+h)$. Since this is never the case when a discontinuity line lies in this interval, this formula cannot be applied blindly to systems with step-index refractive profiles, which is unfortunate as step-index profiles are frequently encountered. It is then usually recommended that discontinuities be placed half-way between consecutive sampling points or that the exact permittivity on every grid point x be replaced with its average on the corresponding mesh, i.e. over the interval $(x-h/2, x+h/2)$. As this paper will demonstrate, the difficulty can be very easily remedied using a proper differentiation formula, without making the subsequent numerical work more difficult and, one no longer has to worry about the respective location of the sampling grid and the discontinuities.

We shall only consider the derivation of scalar normal modes, i.e. the solutions $\psi(x, y)e^{-i\gamma z}$ of the Hemholtz equation

$$(\Delta + k^2n^2(x, y) - \gamma^2)\psi(x, y) = 0 \quad (2)$$

where $k = \omega/c$ and where $n(x, y)$ is the refractive index profile. Two cases are of interest:

Paper 8681J (E13), first received 9th September 1991 and in revised form 2nd January 1992

The author is with the Centre National d'Etudes des Télécommunications, 2, route de Trégastel, BP40, 22301 Lannion, France

(i) The scalar approximation, valid for weakly guiding systems of arbitrary shape, where the field ψ and its normal derivative $\partial\psi/\partial n$ are everywhere continuous.

(ii) The semivectorial approximation, valid for planar systems with discontinuities parallel to either the x or y axes, when the field is linearly polarised along the x or y direction (see the Appendix). Then, if ψ is the transverse electric field, depending on whether the discontinuity line is parallel or normal to the field, either ψ or $n^2\psi$ is continuous; in both cases $\partial\psi/\partial n$ is continuous. There is also an alternative representation where ψ is a magnetic component; then ψ is always continuous while $\partial\psi/\partial n$ can be discontinuous. The classical 3-point formula to be used in such problems is due to Stern [1]; obviously, it is more complex than eqn. 1. It will be derived again and generalised hereafter.

Another important point to be emphasised is that in general one does not want all the modes of a waveguide, but in particular the dominant mode and, more rarely, the next higher mode. There are direct methods to derive these modes, which are more economical than conventional eigenvalue/eigenvector methods in terms of storage and computing time [2]; other methods will be proposed below.

As Seki *et al.* [3] indicated, very little has been published on the accuracy and the reliability of finite difference methods. This cannot be discussed by directly tackling a complex structure such as a rib waveguide and comparing the results with those provided by some approximate method, like the effective-index method. One must first consider basic problems where the exact solution is known, e.g. slab waveguides and circular fibres. Raw results of this kind will be given in this article, demonstrating the performances of classical calculations and their improvement with our new formulae. An application to practical problems with rectangular or rib structure will be given elsewhere.

2 Improved differentiation formulae

2.1 Introduction to 1D formulae

Here we consider the 1D Hemholtz equation, i.e. $(\partial^2/\partial x^2 + k^2n^2 - \gamma^2)\psi(x) = 0$ where the refractive index n is piecewise uniform. The start of the analysis is identical for the scalar and semivectorial cases.

Let us consider the three consecutive points shown in Fig. 1, labelled (-1), (0), (1) and such that the discontinuity lies between points (0) and (1), at distance ξh from point (0) (with $0 \leqslant \xi < 1$). We would like to obtain an expression for the second derivative ψ_0'' at point (0) that would generalise the first-order formula (1). For this we must derive 3rd-order expressions for the fields ψ_{-1} and ψ_1, respectively, at points (-1) and (1). The former is

obviously

$$\psi_{-1} = \psi_0 - h\psi'_0 + \frac{h^2}{2}\psi''_0 - \frac{h^3}{6}\psi'''_0 + O(h^4) \quad (3)$$

The latter is obtained by tracking the field and its derivatives from (0) to (1) across the discontinuity. Let ψ_{d0}, ψ'_{d0}, ψ''_{d0}, ψ'''_{d0} be the field and its first derivatives at the discontinuity, on the (0)-side, and let ψ_{d1}, ψ'_{d1}, ψ''_{d1}, ψ'''_{d1} be

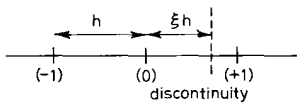

Fig. 1 *Schematics of 3 consecutive grid points with a discontinuity between points 0 and 1*

the corresponding values on the (1)-side. The former quantities are given by

$$\psi_{d0} = \psi_0 + \xi h\psi'_0 + \xi^2\frac{h^2}{2}\psi''_0 + \xi^3\frac{h^3}{6}\psi'''_0 + O(h^4) \quad (4)$$

$$h\psi'_{d0} = h\psi'_0 + \xi h^2\psi''_0 + \xi^2\frac{h^3}{2}\psi'''_0 + O(h^4) \quad (5)$$

$$h^2\psi''_{d0} = h^2\psi''_0 + \xi h^3\psi'''_0 + O(h^4) \quad (6)$$

$$h^3\psi'''_{d0} = h^3\psi'''_0 + O(h^4) \quad (7)$$

The relationship between ψ_{d0} and ψ_{d1} can be expressed as

$$\psi_{d1} = \theta\psi_{d0} \quad (8)$$

where

$$\theta = \begin{cases} 1 & \text{(scalar case)} \\ n_0^2/n_1^2 & \text{(semivectorial case)} \end{cases} \quad (9)$$

The first derivative is always continuous, i.e. $\psi'_{d0} = \psi'_{d1}$. The discontinuity of the second derivative can be obtained from the Helmholtz equation, under either its original form for the scalar case or the equivalent form $n^2\psi'' + (k^2n^2 - \gamma^2)n^2\psi = 0$ for the semivectorial case; in both cases we can write

$$\psi''_{d1} = \theta[\psi''_{d0} + k^2(n_0^2 - n_1^2)\psi_{d0}] \quad (10)$$

The discontinuity of the third derivative can be derived from the derivative of the Helmholtz equation, i.e. $\psi''' + (k^2n^2 - \gamma^2)\psi' = 0$. We obtain

$$\psi'''_{d1} = \psi'''_{d0} + k^2(n_0^2 - n_1^2)\psi'_{d0} \quad (11)$$

Finally, the required field at point (1) is

$$\psi_1 = \psi_{d1} + (1-\xi)h\psi'_{d1} + (1-\xi)^2\frac{h^2}{2}\psi''_{d1} + (1-\xi)^3\frac{h^3}{6}\psi''_{d1} + O(h^4) \quad (12)$$

Inserting eqns. 4–11 into eqn. 12 and putting

$$m = \tfrac{1}{2}k^2(1-\xi)^2(n_0^2 - n_1^2) \quad (13)$$

we can rewrite ψ_1 as

$$\begin{aligned}\psi_1 = {} & [\theta + \theta m h^2]\psi_0 \\ & + [1 - \xi + \theta\xi + mh^2(\theta\xi + (1-\xi)/3)]h\psi'_0 \\ & + [\theta\xi^2 + 2\xi(1-\xi) + \theta(1-\xi)^2]h^2\psi''_0/2 \\ & + [\theta\xi^3 + 3\xi^2(1-\xi) + 3\theta\xi(1-\xi)^2 \\ & \qquad + (1-\xi)^3]h^3\xi'''_0/6 + O(h^4)\end{aligned} \quad (14)$$

2.2 1D scalar case

Eqn. 14 is greatly simplified in the scalar case, since θ then equals 1. The coefficients of $h^2\psi''_0/2$ and $h^3\psi'''_0/6$ are merely 1, so combining this equation and eqn. 3 readily leads to

$$\psi''_0 = \frac{1}{h^2}[\psi_{-1} + \psi_1 - 2\psi_0] - m\psi_0 - \frac{1+2\xi}{3}mh\psi'_0 + O(h^2) \quad (15)$$

The leading terms on the right-hand side are those of the classical formula (eqn. 1); the m terms are corrective terms, of order 0 and 1, respectively, in h. A very simple zeroth-order formula is obtained by dropping the second corrective term, namely

$$\psi''_0 = \frac{1}{h^2}[\psi_{-1} + \psi_1 - (2 + mh^2)\psi_0] + O(h) \quad (16)$$

This formula leads to the same symmetrical tridiagonal structure as eqn. 1 for the matrix representing the discretised second derivative; only the diagonal terms are changed. Though of zeroth-order, the correction is sometimes numerically weak. For instance, in a symmetrical step-index waveguide of width $2a$, its relative magnitude (with respect to the uncorrected diagonal term) is V^2h^2/d^2 where $V^2 = k^2a^2|n_0^2 - n_1^2|$ defines the normalised frequency. With V around 1–2 for single-mode waveguides, the correction is of order $(h/a)^2$, i.e. a small number when there are many grid points inside the guiding layer. However, neglecting it would lead to a sensible error, highly ξ-sensitive, and moreover the case of a symmetrical waveguide is the most favourable. In the case of asymmetric slabs made of a substrate, a weakly guiding layer and air, with the same normalised frequency, the corrective terms of points near the air interface are never negligible.

If one is ready to handle unsymmetrical matrices, one can consider the full equation (eqn. 15). It is transformed into a three-point formula for ψ''_0 by replacing $h\psi'_0$ with $(\psi_1 - \psi_{-1})/2 + O(h^2)$. One obtains explicitly

$$\psi''_0 = \frac{1}{h^2}[\psi_{-1} + \psi_1 - 2\psi_0] - m\psi_0 - \frac{1+2\xi}{6}m(\psi_1 - \psi_{-1}) + O(h^2) \quad (17)$$

A slightly different formula is obtained by replacing $h\psi'_0$ by $\psi_0 - \psi_{-1}$, but it leads to less satisfactory numerical results.

2.3 1D semivectorial case

Since $\theta = n_0^2/n_1^2 \neq 1$ in the semivectorial case, there is no simplification in eqn. 14 and this means that it is impossible to derive a general first-order three-point formula for ψ''_0. We must content ourselves with the formula obtained by dropping the h^3 terms in eqn. 14, namely

$$\psi''_{d0} = \alpha_{-1}\psi_{-1} + \alpha_0\psi_0 + \alpha_1\psi_1 + O(h) \quad (18)$$

where the α coefficients are given by

$$\begin{aligned} D &= [1 - \tfrac{1}{2}(\theta - 1)(2\xi^2 - \xi + 1)]h^2 \\ \alpha_{-1} &= D^{-1}[1 + (\theta - 1)\xi] \\ \alpha_0 &= -D^{-1}[2 + (\theta - 1)(1 + \xi) + \theta mh^2] \\ \alpha_1 &= D^{-1} \end{aligned} \quad (19)$$

It should be noted that the scalar formula (eqn. 16) is recovered by making $\theta = 1$. Also, the Stern three-point formula is again obtained by making $\xi = 1/2$ and $m = 0$, which amounts to neglecting the discontinuity of the second derivative.

2.4 2D scalar case

We now handle the full equation (eqn. 2) with ψ and $\partial\psi/\partial n$ everywhere continuous. The grid points are aligned parallel to the x and y axes but the discontinuity line can have a different direction (see Fig. 2). When this

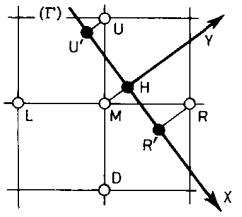

Fig. 2 *Schematics of a discontinuity line* (Γ) *near a grid point M and its four neighbouring points*

line is directed along one axis, say the y-axis, we can evaluate $\partial^2\psi/\partial x^2$ and $\partial^2\psi/\partial y^2$ separately, by means of eqns 16 and 1. The general case of Fig. 2 is more complex.

Let use consider a grid point M near a discontinuity line Γ and let R, L, U and D be the next four grid points as shown in Fig. 2. We introduce X and Y axes directed along Γ and its normal, with an origin H at the nearest point from M. Within an $O(h)$ error, the Laplacian at M can be replaced with the Laplacian at H, on the M-side of Γ and it can be evaluated in the X-Y axes as well as in the initial x-y axes. Obviously, this scheme also means that only a zeroth-order formula will be obtained.

The continuity of ψ, and $\partial\psi/\partial X$ across Γ entails the continuity of $\partial^2\psi/\partial Y^2$ and $\partial^2\psi/\partial X\partial Y$. Among the second-order derivatives, only $\partial^2\psi/\partial X^2$ is discontinuous, with the following jump

$$\begin{aligned}(\partial^2\psi/\partial X^2)_{H,ext} &= (\partial^2\psi/\partial X^2)_{H,int} + k^2(n_{int}^2 - n_{ext}^2)\psi_H \\ &= (\partial^2\psi/\partial X^2)_{H,int} + k^2(n_{int}^2 - n_{ext}^2)\psi_M + O(h) \qquad (20)\end{aligned}$$

where *int* and *ext* stand for internal and external, respectively, i.e. the M-side and the other side.

We now consider second-order Taylor expansions for the field at points M, L, R, U and D in terms of the field and its first and second derivatives at H. The designed Laplacian emerges when forming the classical combination $\psi_L + \psi_R + \psi_U + \psi_D - 4\psi_M$; we finally obtain, with an understood error term $O(h)$

$$\begin{aligned}(\Delta\psi)_M &= (\Delta\psi)_H \\ &= \frac{1}{h^2}(\psi_L + \psi_R + \psi_U + \psi_D - 4\psi_M) \\ &\quad + \tfrac{1}{2}k^2(n_{ext}^2 - n_{int}^2)(\eta_R^2 + \eta_U^2 + \eta_D^2 + \eta_L^2)\psi_M \qquad (21)\end{aligned}$$

where $\eta_R = RR'/h$, i.e. the distance from R to the discontinuity line, divided by h, but only when R is on the external side of the discontinuity, otherwise $\eta_R = 0$; η_L, η_D and η_U are similar normalised distances for L, D and U, nonzero only when these points are on the external side. At most, two of the ηs are not zero, but there can be a single one when the discontinuity is near vertical or horizontal.

2.5 2D semivectorial case

This case is relevant only with linear discontinuities directed along either the x or y axes. One of the derivatives $\partial^2\psi/\partial x^2$ and $\partial^2\psi/\partial y^2$ is always regular and is evaluated with eqn. 1. The other one is obtained using either eqn. 17 or eqn. 18 depending on whether the field is parallel or orthogonal to the discontinuity.

3 Application: scalar calculations

As a first application, we considered the TE_0 mode in a slab waveguide, made of a substrate of index n_{sub}, a core layer of index n_{core} located within $-a < x < a$, and a superstrate of index n_{sup} (with $n_{sup} \leqslant n_{sub}$). The field is analysed in a window $-W < x < W$ with grid points located at $x_p = ph$, $(p = -N, \ldots, N)$ with $h = W/N$, within an assumption of zero field at $x = \pm(N + 1)h$. The Hemholtz equation is thus discretised into a matrix eigenvalue equation such as

$$\boldsymbol{A}\boldsymbol{X} = \gamma^2\boldsymbol{X} \qquad (22)$$

where $\boldsymbol{X}$ is a vector formed with the unknown $\psi(x_p)$ values and where $\boldsymbol{A}$ is a tridiagonal matrix. We first consider zeroth-order calculations with eqn. 16, and also classical calculations with eqn. 1, with or without mesh-averaged permittivities. Then, $\boldsymbol{A}$ is symmetrical, such that $\boldsymbol{A} - k^2n_{core}^2$ is negative definite. Since the dominant mode just corresponds to the highest possible eigenvalue for γ^2, it can be derived by looking for the maximum of the functional

$$F(\boldsymbol{X}) = \boldsymbol{X}^t\boldsymbol{A}\boldsymbol{X}/\boldsymbol{X}^t\boldsymbol{X} \qquad (23)$$

where t indicates the matrix transposition; $\boldsymbol{X}$ is the trial field. This maximum can be conveniently found with a conjugate gradient method, as described in Reference 4. However, it should be noted that such a method converges more rapidly for γ^2 than for the field, because of its stationarity, so that special care must be taken if one is particularly interested in the derivation of accurate fields.

The matrix $\boldsymbol{A}$ becomes unsymmetrical when the first-order formula (eqn. 17) is used. Then there is no simple way to solve eqn. 22 which could be extended to the general 2D case. The preceding maximisation of $F(\boldsymbol{X})$ does not yield the highest eigenvalue of $\boldsymbol{A}$, but that of $\boldsymbol{A} + \boldsymbol{A}^t$.

In the special case of slab waveguides, the rank of the system is at most a few hundreds and a complete diagonalisation can be considered. Another convenient technique is based on the fact that $\boldsymbol{A}$ is tridiagonal and can be made symmetrical by means of a diagonal matrix $\boldsymbol{D}$ such that $\boldsymbol{A}' = \boldsymbol{D}\boldsymbol{A}\boldsymbol{D}^{-1}$ is symmetrical; then eqn. 22 can be rewritten as $\boldsymbol{A}'\boldsymbol{X}' = \gamma^2\boldsymbol{X}'$ with $\boldsymbol{X}' = \boldsymbol{D}\boldsymbol{X}$ and this new equation can be numerically solved with the preceding method. On the other hand, the general $\boldsymbol{A}$ for 2D systems consists of 5 diagonals and cannot so easily be made symmetrical. Furthermore, one must face ranks of several 10^4 or more, preventing any idea of a complete diagonalisation.

Here, we propose an iterated inverse power technique. Let us assume that we have found an approximation γ_0 of the eigenvalue to be found and a (possibly very rough) approximation $\boldsymbol{X}^{(0)}$ for the eigenvector. Then we repeatedly solve

$$(\boldsymbol{A} - \gamma_0^2)\boldsymbol{X}^{(i+1)} = \boldsymbol{X}^{(i)} \qquad (i = 0, 1, 2 \ldots) \qquad (24)$$

Within the seemingly reasonable assumption that the eigenvectors of $\boldsymbol{A}$ map the whole space, one can seen that

$X^{(i)}$ tends towards the eigenvector with the nearest eigenvalue from γ_0^2, i.e. the wanted mode. In practice, we stop the loop as soon as the relative change of $X^{(i)}$ falls below a given threshold related to the designed accuracy for the field. Then the eigenvalue is merely obtained by $\gamma^2 = X^t AX/X^t X$.

The choice of the initial approximation γ_0 is somewhat critical. It must be closer to the exact γ than to the other eigenvalues, but not too close, otherwise eqn. 24 becomes too ill conditioned, leading to numerical difficulties. In the various examples analysed in this article, we obtained good results by adding $0.1k^2\ (n_{core}^2 - n_{sub}^2)$ to the exact value; in real problems, the 'exact' value could be replaced with any fair approximation (Gaussian approximation, effective index method, ...). The starting field can be a very crude approximation such as 0 everywhere except 1 in the middle of the slab, but obviously a better guess resulted in shorter computations. Eqn. 24 was solved by means of a standard library routine for linear systems with a sparse diagonal-like matrix.

The quality of the solution must be estimated from the errors on the eigenvalue and the eigenvector. The former is put in a normalised form by replacing γ with the following normalised propagation constant

$$B = \frac{(\gamma/k)^2 - n_{sub}^2}{n_{core}^2 - n_{sub}^2} \tag{25}$$

As B varies between 0 and 1 and is larger than 0.1–0.2 under normal operation, the difference between the computed value of B and its exact value can be considered to be a normalised figure for the accuracy on the propagation constant. With regard to the field, we have considered the mean quadratic error ε_F, which can be defined as

$$\varepsilon_F = \{2 - 2(X^t X_{ex})/[(X^t X)(X_{ex}^t X_{ex})]^{1/2}\}^{1/2} \tag{26}$$

for unnormalised fields.

Typical convergence plots for $B - B_{ex}$ and ε_F are shown in Figs. 3 and 4, respectively, for a strongly asymmetrical waveguide and for a nearly symmetrical waveguide, with identical substrate and superstrate but with a two-layer core. We included the second case for completion and also because we disagree with the data published elsewhere [3] (we found that the classical results were far more accurate than was reported). The following conclusions can be drawn:

(i) Classical calculations are considerably improved by using mesh-averaged permittivities.

(ii) Using the new zeroth-order formula does not bring a decisive advantage over the classical calculation with mesh-averaged permittivities, at least in this special case. At most, the oscillating behaviour is strongly reduced (it should be noted that these oscillations are related with the strong asymmetry of the waveguide; they nearly vanish for symmetrical waveguides).

(iii) The accuracy is notably improved by using the first-order formula, especially on field calculations.

It can also be observed that the limits for B lie between the 0th and the first-order results, at least in these two figures. However, these limits are not necessarily the exact values, due a possible windowing error (see Section 5).

It is interesting to note the density of the sampling beyond which the errors fall below 10^{-3}. When various 'rigorous' methods for deriving guided modes in complex waveguides are compared, one often notes that they differ by several 10^{-3} for B [5]. It would therefore be important to ascertain whether the third digit of B can be considered reliable for a given method; unfortunately, this information is generally not available. Figs. 3 and 4 give

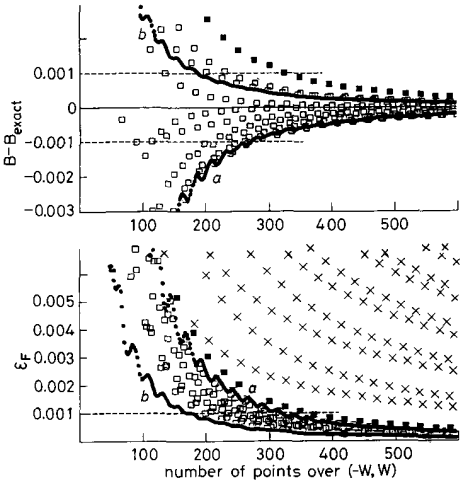

Fig. 3 *Error curves for TE_0 mode of an asymmetrical slab 0.5 μm wide. Field is analysed in a window $(-W, W)$ with $W = 3$. Points and curves display dependence of errors on total number of grid points*

$\lambda = 1.55$ μm
Substrate refractive index 3.17
Guiding layer refractive index 3.512
Superstrate refractive index 1.0
× classical calculation, using eqn. 1 without mesh averaging
□ classical calculation, using eqn. 1 with mesh averaging
■ classical calculation discontinuities halfway between grid points
a new zeroth-order calculations
b new first-order calculations

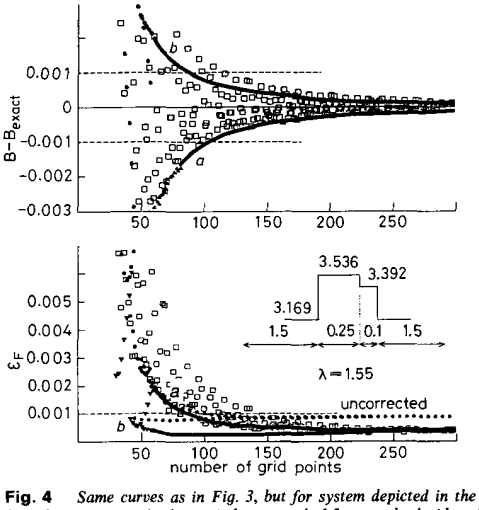

Fig. 4 *Same curves as in Fig. 3, but for system depicted in the inset. Lengths are in μm. Analysis window extends 1.5 μm on both sides of core. All the curves were obtained with the boundary correction described in Section 5, except the dotted line labelled 'uncorrected' in ε_F diagram. The correction seems to have no effect on the B values in this special case. Curves a and b break into isolated points for less than 70–80 grid points; this corresponds to only 2 points in smaller core layer*

some indication for the finite difference techniques, at least in the particular cases considered. The 10^{-3} threshold for B error is obtained with about 20 points inside the core in Fig. 3, and with only 10 in Fig. 4 (in spite of

the internal core discontinuity in this case); probably the former case is more difficult because of the strong asymmetry between the discontinuities. However, another important parameter is the effect of a nonzero field on

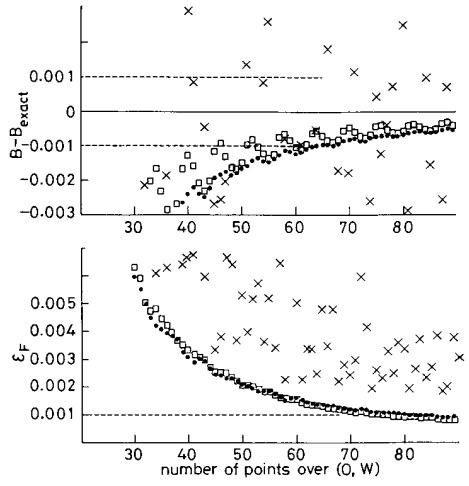

Fig. 5 *Error curves for LP_{01} mode of a circular fibre of radius R, analysed in a square window $(-W, W) \times (-W, W)$, with $W = 6R$, for a normalised frequency $V = 2.35$.*

× classical calculation, without mesh averaging
□ classical calculation with mesh averaging
● new method using eqn. 21

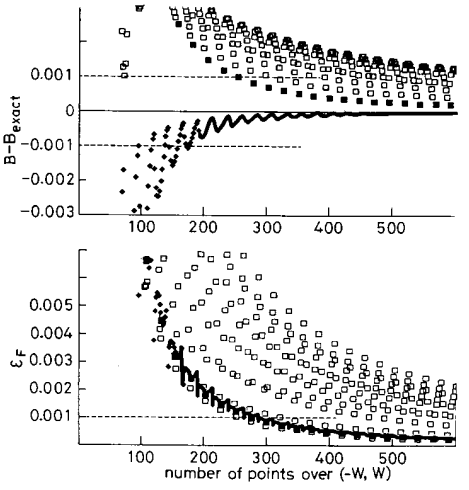

Fig. 6 *Same curves as in Fig. 3, for same slab waveguide, but for TM_0 mode*

□ classical calculation with mesh averaging
■ original Stern calculation
~·· new zeroth-order calculation

the edge of the analysis window and its possible correction. We shall return to this point later.

3.1 A 2D scalar example

Fig. 5 displays similar results for $B - B_{ex}$ and ε_F in the case of the LP_{01} mode in a circular fibre. Abscissae are now graduated with the number of grid points over the half-side of the window, so that, for example 80 points correspond to a rank $161 \times 161 = 25921$ for the full window. Fortunately, the conjugate gradient method converges very rapidly; a few hundreds of iterations are sufficient to obtain the results plotted in the figure. The conclusions are the same as for the slab case. It is necessary to take averaged permittivities in the classical calculation. The new method then leads to equivalent results.

4 A semivectorial example: slab TM_0 mode

Convergence plots are displayed in Fig. 6, for the TM_0 mode of the same waveguide as in Fig. 3. The solid curves are obtained using the new formula (eqn. 18). The square dots correspond to a Stern-like calculation with averaged permittivities, while solid square dots correspond to Stern's original calculation, with discontinuities half-way between the grid points. The B estimations are clearly more accurate with the new method than with classical methods. The best classical results are given by the original Stern calculation. Moving the grid points with respect to the discontinuities can make the error on B increase up to 5 to 10 times the error with the new method.

When comparing Figs. 3 and 6 it should be noted that curiously the B-curves converge quite more rapidly for the TM mode than for the TE mode. However, there is nothing similar for the field error.

5 Correcting the windowing error

In all the preceding calculations, the window size was large enough to satisfy the requirement of a negligible field on its boundary (a few 10^{-5} of the field on the centre). To some extent, computation with such a large window is a waste of memory and CPU time and it is natural to try to relax this requirement, by replacing the boundary condition $\psi = 0$ with

$$\frac{\partial \psi}{\partial n} = -\kappa\psi = -(\gamma^2 - k^2 n_{ext}^2)^{1/2}\psi \tag{27}$$

In slab problems with grid points at $x_p = ph$ ($p = -N, \ldots, N$), this condition is implemented by writing $\psi_{N+1} = \psi_N \exp(-\kappa h)$, hence

$$\psi''_N = \frac{1}{h^2}[\psi_{N-1} - (2 - e^{-\kappa h})\psi_N] \tag{28}$$

and a similar form for ψ''_{-N}.

Eqn. 27 is exact in the case of slab problems and indeed, in our numerical trials, we could always obtain errors well below 0.001 for B and for the field, even when the field on the boundary was 20% of its maximum value.

But eqn. 27 is only approximate for 2D problems. It then reads as either $\partial\psi/\partial x = -\kappa\psi$ or $\partial\psi/\partial y = -\kappa\psi$ while the exact boundary condition in the special case of a circular fibre should be $\partial\psi/\partial r = -\kappa\psi$. This approximation then induces specific errors that should be estimated; Fig. 7 yields some information about them. It displays convergence curves similar to those of Fig. 5, for ratios $W/R = 3$, 2 and 1.5 instead of 6 in Fig. 5. The field at $r = W$ is 0.009, 0.058 and 0.155, respectively, (for a value 1 at $r = 0$). It is clear that too narrow a window leads to degraded B and ψ. The field error increases more rapidly than the B error. Also the (relatively) poor derivation of the field must be combined with a necessary extrapolation outside the window, that could be still

more hazardous. In conclusion, results corresponding to a field on the boundary of a few percents of its maximum value should be reliable within a 10^{-3} relative error. More than 10% could induce a sensible degradation, specially on the field.

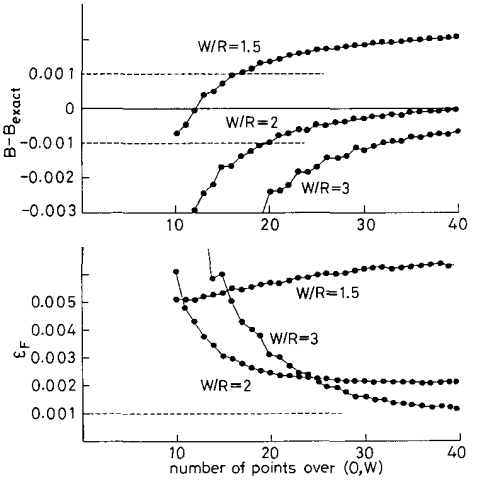

Fig. 7 *Error curves for LP_{01} mode of a circular fibre, with $V = 2.35$, for various widths of analysis window (W = half-width). Boundary condition is given by eqn. 27*

6 Conclusions

We have investigated the accuracy of finite difference formulae using uniformly spaced grids for the derivation of scalar or semivectorial fields. The classical 3-point formula for scalar fields, which is usually a first-order formula (i.e. the error is of order h^2) when the second derivative is continuous, contains a zeroth-order error when the refractive index is discontinuous. New formulae have been given, of zeroth- or first-order, irrespective of the location of the discontinuity with respect to the grid points.

A new formula has been given for the semivectorial fields of zeroth-order whatever the location of the discontinuity may be. There cannot be first-order 3-point formula. The interest of the new formulae with respect to the previous works has been demonstrated by analysing the errors on the propagation constants and the fields of dominant modes in slab waveguides or in circular fibres. The effectiveness of the boundary condition based on an exponential decay of the field outside the analysis window was also discussed.

7 References

1 STERN, M.S.: 'Semivectorial polarised H-solutions for dielectric waveguides with arbitrary index profiles', *IEE Proc. J, Optoelectron*, 1988, **135**, pp. 333–338

2 STERN, M.S.: 'Rayleigh quotient solution of semivectorial field for optical waveguides with arbitrary index profiles', *IEE Proc. J., Optoelectron.*, 1991, **138**, pp. 185–190

3 SEKI, S., YAMANAKA, T., and YOKOYAMA, K.: 'Two-dimensional analysis of optical waveguides with a nonuniform finite difference method', *IEE Proc. J, Optoelectron.*, 1991, **138**, pp. 123–127

4 PRESS, W.H., FLANNERY, B.P., TEUKOLSKY, S.A., and VETTERLING, W.T.: 'Numerical recipes' (Cambridge University Press, Cambridge, 1986)

5 VASSALLO, C., and WANG, Y.H.: 'A new semirigorous analysis of rib waveguides', *J. Lightwave Technol.*, 1990, **LT-8**, pp. 56–64

6 VASSALLO, C.: 'Optical waveguide concepts' (Elsevier, Amsterdam, 1991)

8 Appendix: validity of the semivectorial assumption

Optical waveguides that are currently of interest are weakly guiding dielectric structures. Their refractive index has little variation around a reference value n_0 inside a domain which can either be the whole x–y plane (optical fibres, rectangular waveguide) or is surrounded with an exterior region where the refractive index is markedly lower than n_0 (rib or ridge waveguides embedded in the air). Such structures can be analysed in terms of the theory of weakly guiding waveguides embedded in low index material [6]. Their vectorial modes are close to combinations of degenerate LP modes linearly polarised along x and y axes and they are themselves polarised along these directions only when the coupling terms between these LP modes vanish. One easily verifies that this occurs when the waveguide is symmetrical with respect to the x or y axis, and also in planar waveguides where all the discontinuities are either parallel or orthogonal to axes. Only the latter case is considered in this paper; the relevant continuity relation which should be applied to semivectorial fields across discontinuity lines which are neither parallel nor orthogonal to the field is currently unclear.